Stem Cell Reports
Resource
ISSCR
OPEN ACCESS

Production of large, defined genome modifications in rats by targeting rat embryonic stem cells

Jeffrey Lee,[1,*] Jingjing Wang,[1] Roxanne Ally,[1] Sean Trzaska,[1] Joseph Hickey,[1] Alejo Mujica,[1] Lawrence Miloscio,[1] Jason Mastaitis,[1] Brian Morse,[1] Janell Smith,[1] Amanda Atanasio,[1] Eric Chiao,[1] Henry Chen,[1] Adrianna Latuszek,[1] Ying Hu,[1] David Valenzuela,[1] Carmelo Romano,[1] Brian Zambrowicz,[1] and Wojtek Auerbach[1]
[1]Regeneron Pharmaceuticals, Tarrytown, NY 10591, USA
*Correspondence: jeffrey.lee@regeneron.com
https://doi.org/10.1016/j.stemcr.2022.11.012

SUMMARY

Rats were more frequently used than mice to model human disease before mouse embryonic stem cells (mESCs) revolutionized genetic engineering in mice. Rat ESCs (rESCs) were first reported over 10 years ago, yet they are not as frequently used as mESCs. CRISPR-based gene editing in zygotes is widely used in rats but is limited by the difficulty of inserting or replacing DNA sequences larger than about 10 kb. We report here the generation of germline-competent rESC lines from several rat strains. These rESC lines maintain their potential for germline transmission after serial targeting with bacterial artificial chromosome (BAC)-based targeting vectors, and CRISPR-Cas9 cutting can increase targeting efficiency. Using these methods, we have successfully replaced entire rat genes spanning up to 101 kb with the human ortholog.

INTRODUCTION

Genetic engineering enables the production of disease-associated genotypes in model animal systems, especially mice (White et al., 1995; Yue et al., 2006). Complex modifications can be combined to expand the power of these models, as in immunodeficient models to study hematopoiesis and tumor biology (Mashimo et al., 2012; Rongvaux et al., 2013; Strowig et al., 2011). CRE-loxP and Tet-inducible systems enable conditional inactivation or regulation of endogenous genes or transgenes with a wide range of functions (Aiba and Nakao, 2007; Jaisser, 2000; Lau et al., 2011).

Gene humanization—the replacement of an endogenous gene with its human counterpart—enables the testing of human monoclonal antibodies in mice for functional activity in a preclinical system, which accelerates the development of new therapies (Gusarova et al., 2015; Macdonald et al., 2014; Murphy et al., 2014; Stein et al., 2012; Waite et al., 2020). One example is neurotrophic receptor kinase 2 (NTRK2), a promising target for neuroprotection in degenerative eye diseases such as glaucoma. NTRK2 is a widely distributed neurotrophic receptor in the brain and is highly expressed in the retina (Chao, 2003). Binding of brain-derived neurotrophic factor (BDNF) to NTRK2 triggers its dimerization, autophosphorylation, and activation of neuroprotective signaling pathways (Bai et al., 2010). NTRK2 is therefore a potential therapeutic target for activation by agonist antibodies.

Historically, the most powerful technology for genetic engineering in mice has been embryonic stem cells (ESCs) (Bronson and Smithies, 1994; Capecchi, 1989; Smith, 2001). ESCs are pluripotent self-renewing cells that, when transplanted into preimplantation embryos, contribute to the development of every cell type in the animal, including germ cells, which allows the propagation of genetic modifications to future generations. High-quality ESCs can be sequentially engineered to produce cells with multiple mutations or with large modifications that span several million base pairs (Murphy et al., 2014). Until recently, ESC-based genetic engineering was done exclusively in mice, the only organism for which ESCs were available. Mouse ESCs (mESCs) were first isolated decades ago (Evans and Kaufman, 1981; Martin, 1981); soon after, modified mESCs were used to produce mice carrying targeted mutations (Doetschman et al., 1987; Robertson et al., 1986; Thomas and Capecchi, 1987; Zijlstra et al., 1989). Since then, mice have become the predominant animal system for modeling disease using genetic engineering.

Rats have been used for laboratory studies for over 150 years (Baker et al., 1979; Jacob, 2010). Prior to the discovery of mESCs, rats were the model of choice for certain fields of research (Amos-Landgraf et al., 2007; Jacob, 2010; Morrison et al., 2008). As genetic engineering began to drive mammalian research, rats fell behind due to a lack of rat ESCs (rESCs). Many attempts to apply mESC derivation techniques to the derivation of rESCs have failed (e.g., Brenin et al., 1997; Li et al., 2009). The first genuine rESCs were reported in 2008; these cells possess the same properties as mESCs (Buehr et al., 2008; Li et al., 2008). However, rESCs have only rarely been used for gene targeting (Meek et al., 2010; Men et al., 2012; Tong et al., 2010). With the advent of gene editing in 1-cell embryos, especially clustered regularly interspaced

Table 1. Derivation of euploid rESC lines using variations on 2i culture media prior to plating

Strain	Source	Stage	Embryos	Media to blast	Media to plating	Days to plating	Plated	Out growths	Lines (% versus plated)	Karyo typed (P7)	Euploid
DA	cryo'd embryos	8-cell (e2.5)	11	KSOM + 2i	2i	3	9	3	3 (33)	2	2
DA	cryo'd embryos	8-cell (e2.5)	11	mR1ECM + 2i	2i	2	11	7	6 (54)	4	4
BNSDF1	cryo'd embryos	8-cell (e2.5)	43	mR1ECM + 2i	2i	2	28	18	12 (43)	12	10
ACI	superov. females	blastocyst (e3.5)	19	N/A	mR1ECM +2i	1	11	7	6 (54)	3	2

All embryos that appeared healthy were plated on the specified day, including those that had not yet cavitated. Karyotypes were performed at P7. Cryo'd, cryopreserved; superov., superovulated. See also Table S1.

short palindromic repeats (CRISPR-Cas9)-based editing, genetic manipulation in rats has become easier, and many labs have adopted this approach (Menoret et al., 2010; Vaira et al., 2012). Thus, rESC technology has not been developed to its full potential. However, there are significant limitations to current gene-editing technologies, including the production of imprecise or unwanted mutations and a severe limit on the size of knockin or replacement modifications that rely on homologous recombination. This effectively makes complex modifications such as gene humanization impossible unless the gene of interest is very small. Thus, for certain applications, gene editing in embryos is not feasible, and the use of ESCs is required.

We set out to establish an rESC-based gene-targeting platform like our mESC-targeting pipeline (Valenzuela et al., 2003) in order to use rats to model human diseases. Here, we present data demonstrating that rESCs can be targeted to produce large genome modifications, that they can be sequentially targeted, that CRISPR-Cas9 technology can be used to improve targeting efficiency, and that genetically modified rats can be produced using rESCs. We provide data from several examples, including the humanization of the rat *Ntrk2* gene as a demonstration of this technology. Activation of the humanized NTRK2 receptor by agonist antibodies shows no neuroprotective effect in the retinas of humanized *Ntrk2* (*hNtrk2*) mice; in contrast, NTRK2 activation in *hNtrk2* rats shows a strong neuroprotective effect.

RESULTS

rESC derivation and characterization

We developed our methods for deriving rESCs by testing the effects of genetic background, embryo source (fresh collected versus cryopreserved), stage (8-cell to blastocyst), and culture media on derivation efficiency (Tables 1 and S1). We derived lines from the inbred Dark Agouti (DA) and August Copenhagen Irish (ACI) rat strains as well as F1 hybrid crosses between Brown Norway and Sprague Dawley (BNSDF1). Derivation efficiency was similar for all backgrounds tested: about one line per 2–4 embryos (Table S1). We also derived lines from frozen and fresh embryos, as well as from 8-cell-, morula-, and blastocyst-stage embryos (Tables 1 and S1). Again, efficiencies were similar, with slightly higher rates using earlier-stage embryos.

We reasoned that culturing the embryos, prior to plating, in the "2i" inhibitors PD0325901 (MEK-1/2 inhibitor) and CHIR99021 (GSK-3β inhibitor) (Buehr et al., 2008; Ying et al., 2008) might prime the inner cell mass to remain undifferentiated upon plating and thereby improve derivation efficiency. Indeed, when we cultured preblastocyst-stage embryos in standard mouse (KSOM) or rat (mR1ECM) embryo culture media supplemented with the 2i inhibitors, we produced 71 outgrowths from 138 embryos (51%) and recovered 57 cell lines (80% of outgrowths, 41% of embryos; Table S1). However, culturing DA embryos to the blastocyst stage in standard 2i media supplemented with the ROCK inhibitor Y-27632 produced no ESC lines (Table S1). We concluded that our best conditions for efficient rESC derivation were to culture embryos overnight from the 8-cell stage to blastocyst in mR1ECM + 2i inhibitors, followed by overnight culture in 2i media and plating onto mouse embryonic fibroblasts (MEFs; Tables 1 and S1). The most important steps in our hands were to start with earlier-stage embryos and to culture preblastocyst-stage embryos in media that had been validated for early embryo culture (KSOM or mR1ECM).

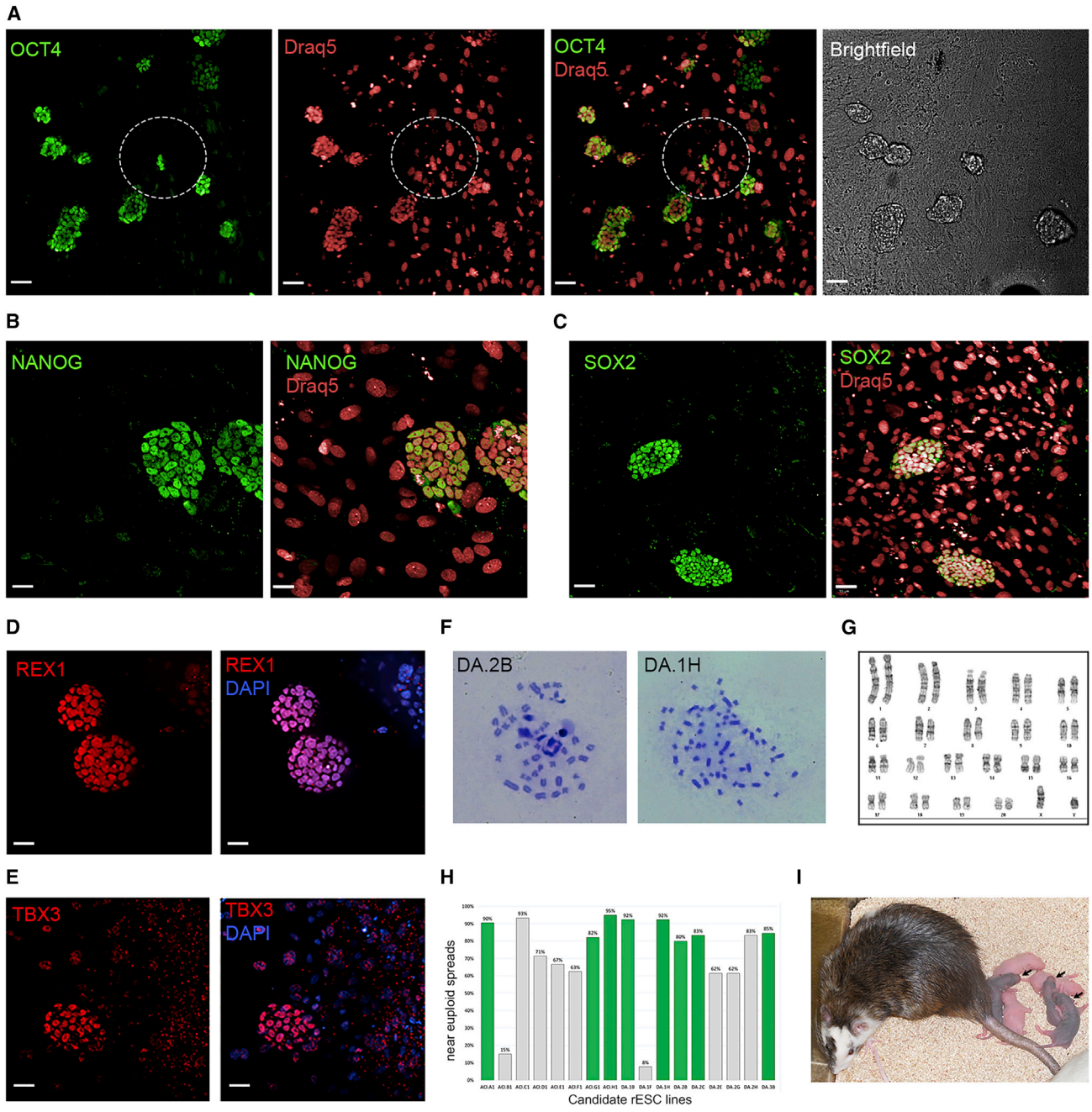

Figure 1. rESC characterization

Parental rESC colonies (line DA.2B) were cultured on mitotically inactivated mouse embryonic fibroblasts (A–E). All stainings were performed in duplicate on separate cultures.

(A) OCT4 (green), nuclear marker DRAQ5 (red), overlay, and bright field. rESC colonies appear as tightly packed clusters of nuclei; separated nuclei are from MEFs (red nuclei in circle).

(B) NANOG (green) and DRAQ5 (red).

(C) SOX2 (green) and DRAQ5 (red).

(D) REX1 (red) and nuclear marker DAPI (blue).

(E) TBX3 (red) and DAPI (blue).

(F) Metaphase spreads from line DA.2B (~42 chromosomes) and DA.1H (~64 chromosomes).

(legend continued on next page)

Our rESC lines formed compact undifferentiated spherical colonies with tight cell-cell boundaries and a high nuclear-to-cytoplasmic volume ratio (Figures 1A–1E). The colonies were very loosely adherent or non-adherent to MEFs. We attempted to subclone several lines to produce fully adherent lines, but after 3 passages, we still consistently saw a mix of adherence phenotypes (data not shown). We concluded that variable adherence to MEFs is an intrinsic property of the cells and may be affected by external influences like colony size, media volume in the well, and the frequency of plate handling.

rESCs are reported to become aneuploid during culture (Buehr et al., 2008; Li et al., 2008). We evaluated our lines by counting chromosomes in metaphase spreads (Figures 1F and 1H; Table S2). Lines in which at least 80% of the spreads contained less than 46 chromosomes were scored as "near euploid" (the euploid rat karyotype is 42); these lines were fully karyotyped. We identified multiple euploid lines from the ACI and DA backgrounds (Tables 1 and S1; Figure 1G).

Standard pluripotency markers such as POU5F1 (OCT4), NANOG, SOX2, REX1, TBX3, alkaline phosphatasem, and KLF4 were expressed at high levels in all lines examined (Figure 1; data not shown). Some lines showed mixed morphologies consisting of small, compact colonies surrounded by large, flat cells in a tiled pattern. We assayed GATA6 expression, a marker of extraembryonic endoderm (Chazaud et al., 2006), and found expression in the flattened peripheral cells but not in the rESC colonies (data not shown); however, we did not further characterize these lines.

The ultimate test of pluripotency for ESCs is germline transmission (GLT) following microinjection into early-stage embryos. We microinjected rESCs from multiple lines into blastocysts from the albino SD strain. We produced chimeras from these injections, and these chimeras sired agouti pups, demonstrating GLT of the rESC genome (Figure 1I; Table 2).

Targeted modifications in rESCs

We produced targeted rESCs clones using plasmid-based small targeting vectors (STVECs; having homology arms <10 kb long) to make small modifications, including deletions of the *Apoe* and *Il2rg* genes and insertion of a lacZ reporter transgene into the *Gt(ROSA)26Sor* (*Rosa26*) locus (Figure S1). We achieved targeting efficiencies in the range of 1%–6% as determined by TaqMan-based qPCR (Tables 3 and S5).

Next, we used bacterial artificial chromosomes (BACs) from a library prepared with genomic DNA from our DA2B rESC line to build BAC-based large targeting vectors (LTVECs; having homology arms >10 kb long) as previously described (Valenzuela et al., 2003). LTVECs contain homology arms up to 90 kb in length and are designed to delete or replace up to 100 kb of a sequence (Figure S1; Table S6). We achieved targeting efficiencies with LTVECs comparable to similar projects in mESCs, including an 86 kb deletion and a 79 kb insertion (Table 3).

We next tested the ability of site-specific nucleases such as zinc-finger nucleases, TALENs (data not shown), and the CRISPR/Cas9 system to enhance targeted recombination. Using CRISPR-Cas-9 and gene-specific single guide RNAs (sgRNAs; Table S4) that target within the gene of interest, we achieved large modifications of up to 100 kb (replacement of the rat *Hc* gene with the human *HC* gene, a 101 kb humanization; Table 3). CRISPR-assisted targeting efficiencies for these projects ranged from 6% to 60%. In all cases where we compared LTVEC targeting efficiency with and without CRISPR, targeting efficiency improved with the addition of CRISPR (Table 3). We also sequentially targeted rESCs to produce multiply targeted clones (deleting the *Rag1* and *Rag2* genes in a clone that had a previously targeted deletion at the *Il2rg* locus) or to re-target previously modified loci (insertion of the human *C1Q* and *C3* genes at the previously deleted rat *C1Q* and *C3* loci; Table 3). Targeting efficiency in these projects was comparable to single-targeted clones. In two cases (the *C3* and *Hc* humanizations), we only produced targeted clones when we included CRISPR-Cas9 (Table 3).

Production of modified rat lines by rESC microinjection and chimera breeding

We tested GLT of single-targeted rESC clones by microinjection into SD blastocysts. Forty-three targeted clones were injected; 23 produced chimeras that transmitted the targeted mutation to F1 progeny (56%; Tables 2 and S3). Among the 23 transmitting clones, 38 of the 48 chimeras (70%) transmitted the rESC genome through the germline (Table 2). For the transmitting chimeras, the overall GLT rate (defined as the number of ESC-derived pups compared with the total number of pups produced by each chimera) was 12.6%, similar to the transmission rate for the unmodified parental rESCs. We concluded that the processes of expansion, electroporation, clonal plating, and drug selection did not negatively impact the cells' pluripotency.

(G) DA2B karyotype and passage P4 (42, X,Y).
(H) Summary of chromosome counts for 17 rESC lines.
(I) Male chimera produced by microinjection of ACIG1 parental cells, with 6 F1 pups; 3 pups are agouti (arrows).
Scale bars are 50 (A) and 20 mm (B–E).
See also Table S2.

Table 2. Germline transmission of parental rESC lines and targeted clones

Parental rat ESC lines

Cell line	Genetic background	Blasts injected (1 surrogate each)	Pups	Male chimeras	Germline-transmitting chimeras	From germline-transmitting chimeras			
						Litters	Pups	ESC-derived pups	GLT rate (%)
DA.2B (XY parental line)	DA	10	4	3	2	6	69	8	11.6
		13	7	2	1	3	35	3	8.6
		13	0	0	0	0	0	0	0
ACI.G1 (XY parental line)	ACI	20	11	2	0	0	0	0	0
		15	8	3	3	9	103	11	10.7
DA.2C (XX parental line)	DA	15	6	3 (female)	2 (female)	2	29	7	24
		15	2	0	0	0	0	0	0

Single targeted clones

Clones injected	Chimeras bred	GLT chimeras (%)	Litters	Pups	ESC-derived pups	GLT rate (%)
20	48	32 (67)	224	2,515	260	10.3
Transmitting chimeras (n = 32) →			173	1,952	260	13.3
Non-transmitting chimeras (n = 16) →			51	563	0	0

Sequentially targeted clones

Clones injected	Chimeras Bred	GLT chimeras (%)	Litters	Pups	ESC-derived pups	GLT rate (%)
3	6	6 (100)	24	306	25	8.2

Germline transmission of targeted clones broken down by litter

Litter number	1	2	3	4	5	6
Chimeras with 1st germline transmission in this litter (n = 38 chimeras)	21	9	2	6	0	0
Early founder rate (%)	55	24	5	16	N/A	N/A
Cumulative founder rate (%)	55	79	84	100	N/A	N/A

For parental lines DA2B and ACIG1, all male chimeras were test bred. For parental line DA2C, all female chimeras were test bred. Single targeted clones were produced by electroporation of targeting vectors into the parental cell lines DA2B or ACIG1. Sequentially targeted clones were produced by electroporation of targeting vectors into previously targeted clones. GLT of the 38 chimeras from gene targeting is broken down by litter. See also Table S3 and Figure S2.

We also tested GLT for three sequentially targeted clones. Targeted clones that had previously shown GLT were targeted a second time, undergoing the same processes as the first time and increasing the passage number. The GLT rate for re-targeted clones was 8.2%, a slight reduction compared with single-targeted clones (13.3%; Table 2). However, the transmission rate for each re-targeted clone was similar to the rate for its single-targeted parental clone (Table S3), confirming that the pluripotency of these cells is not strongly diminished by the processes required to target genes.

We also collected data on GLT (yes or no) and the extent of coat-color chimerism for 119 male chimeras produced by rESC microinjection. Ninety-nine chimeras were scored as $\geq$80% coat-color chimerism, but only 42 showed GLT (Figure S2). Among 20 chimeras with <80% coat-color chimerism, 10 showed GLT (Figure S2), including 2 that were scored as 10% chimerism. We also analyzed the timing of GLT by litter. Twenty-one of 38 transmitting chimeras (55%) produced at least one germline pup in the first litter, and all of the transmitting chimeras produced at least one germline pup in the first four litters (Table 2). Since our objective with each project is to achieve GLT, we established a standard practice of test breeding all male chimeras up to the fourth litter.

Rat *Apoe* knockout phenotype

APOE is major cholesterol transporter and has been linked to cardiovascular disease, including atherosclerosis (Daniels et al., 2009). *Apoe* knockout (KO) mice show progressive increases in serum cholesterol and low-density lipoprotein (LDL) and form extensive aortic plaques (Meir and Leitersdorf, 2004; Nakashima et al., 1994). However, mice have limitations as models for cardiovascular disease. The small blood volume in mice makes longitudinal serum measurements difficult, and some highly informative techniques such as RNA sequencing (RNA-seq) analysis of the aortic endothelial layer are challenging due to the small tissue sample available. *Apoe* KO rats could overcome these limitations.

We designed an STVEC to delete the coding region of the *Apoe* gene and replace it with a *lacZ* reporter inserted at the start of the *Apoe* coding sequence (Figure 2A). Targeting was confirmed by TaqMan and junction PCRs (Figures 2B and S3). *Apoe* KO rats expressed LacZ throughout the liver (Figures 2E and 2F), mimicking the endogenous ApoE RNA expression pattern (Massimi et al., 1999). We measured serum cholesterol, LDL, and high-density lipoprotein (HDL) in *ApoE* homozygous KO (Hom; $Apoe^{-/-}$), heterozygous (Het; $Apoe^{+/-}$), and wild-type (WT) rats from 6 to 60 weeks of age (Figures 2J–2L). *Apoe* KO rats had severely elevated serum cholesterol at 6 weeks of age, whereas heterozygotes showed no elevation. Over time, serum cholesterol concentration partially recovered and eventually reached a steady state of about 2–3 times above the WT. This differs from *Apoe* KO mice, which show steady increases in serum cholesterol throughout life (Plump et al., 1992). Serum LDL in *Apoe* KO rats was 2–3 times higher than in the WT and Het rats from 6–32 weeks of age. Serum HDL concentration in the KO rats remained constant throughout the course of the study at 4–5 times lower than that in WT rats, while the *Apoe* Het rats maintained HDL levels intermediate between those in the KO and WT animals. Finally, we examined the aortas of the KO rats at 32 weeks but found virtually no evidence of atherosclerotic plaques compared with WT rats (Figures 2G and 2H), in stark contrast to mouse *Apoe* KOs (Figure 2I).

Production of immunodeficient rats: *Il2rg*, *Rag1*, and *Rag2* KOs

Mice and rats with deletions of the *Prkdc*, *Rag1*, *Rag2*, and *Il2rg* genes show immune disorders associated with dysfunction in T, B, and natural killer (NK) cells (Mashimo et al., 2012; Walsh et al., 2017; Zhao et al., 2019). To generate immunodeficient rats, we deleted the *Il2rg* coding region with an STVEC (Figures 3A and 3B; Table 3) and confirmed GLT of a targeted clone. We also deleted 16.6 kb of the *Rag1* and *Rag2* genes, the intergenic region between them (Figures 3A and 3B; Table 3), and then interbred these lines to produce RG (*Rag1/Rag2/Il2rg*) triple KO rats. We characterized the individual KOs and the triple KOs by fluorescence-activated cell sorting (FACS). *Il2rg* KO and *Rag1/2* KO rats had hypoplastic thymuses and decreased spleen weights compared with WT control animals (Figure 3C; data not shown), as well as decreased circulating B and T cells, compared with WT controls (data not shown). *Il2rg* KO rats also lacked circulating NK cells, whereas the NK cell population in *Rag1/2* KO rats was increased (data not shown). FACS analysis of RG rats confirmed severe reductions in all cell populations analyzed (Figures 3D and 3E).

Humanization of the *Ntrk2* locus

NTRK2 is a receptor tyrosine kinase and is the primary receptor for BDNF signaling in the retina (Chao, 2003). BDNF activity is neuroprotective, and NTRK2 activation may protect against photoreceptor loss and blindness in conditions like glaucoma. BDNF application has only mild temporary neuroprotective effects in mouse models of glaucoma, likely because BDNF also activates the P75 receptor, which triggers apoptosis. NTRK2 activation by an agonist antibody could potentially be neuroprotective. However, application of NTRK2 agonist antibodies in a *hNtrk2* mouse optic nerve transection model had no effect on retinal ganglion cell loss (Figures 4H and 4I).

Table 3. Target gene modifications in rESCs

Targeting vector only

Gene	Cell line	Vector size (kb)	Modification	Insertion/deletion size (kb)	Colonies screened	Colonies targeted	Targeting rate (vector only) (%)	Targeting rate (vector + CC9)
Il2rg	DA.2B	16	deletion	6/3.2	80	42	52.5	N/A
Chr14 target A	DA.2B	137	humanization with point mutation	25.2	143	70	49	N/A
Rag1/Rag2	DA.2B	139	deletion	8.7/16.6	89	42	47.2	N/A
Chr14 target A	DA.2B	137	humanization	25.2	96	19	19.8	N/A
Chr7 target A	DA.2B	141	point mutation	N/A	92	10	10.9	N/A
Rosa26	ACI.G1	18	deletion	6/0.117	96	6	6.3	N/A
Rosa26	DA.2B	18	deletion	06/.117	96	2	2	N/A
Rag1/Rag2[a]	*Il2rg* KO	150	deletion	16.6	90	1	1.1	N/A

Targeting vector ± CRISPR

Gene	Cell line	Vector size (kb)	Modification	Insertion/deletion size (kb)	Colonies screened (±CRISPR)	Colonies targeted (±CRISPR)	Targeting efficiency (vector only) (%)	Targeting efficiency (vector + CC9) (%)
C3[a]	*C3* KO	188	humanization	48/25	17/84	0/10	0	11.9
Hc	DA.2B	141	humanization	101/86	176/176	0/46	0	26.1
Il2rg	DA.2B	19	humanization	9.8/3.2	77/84	46/54	59.7	64.3
ApoE	DA.2B	21	deletion	8.4/1.9	75/80	32/42	42.7	52.5
Hc	DA.2B	48	deletion	8/86	88/88	5/14	5.7	15.9
C3	DA.2B	148	deletion	8.5/24.7	33/71	2/22	6.1	31
Ntrk2	DA.2B	141	humanization	79/69	288/288	1/22	0.4	7.6

Targeting Vector + CRISPR

Gene	Cell line	Vector size (kb)	Modification	Insertion/deletion size (kb)	Colonies screened (+CC9)	Colonies targeted (+CC9)	Targeting rate (vector + CRISPR)	Targeting rate (vector + CRISPR) (%)
C1Q	DA.2B	151	deletion	8.4/17.5	72	23	N/A	31.9
Chr7 target A	DA.2B	129	humanization	23	176	40	N/A	22.7
Ntrk2	DA.2B	62	humanization	77	54	11	N/A	20.4
Chr13 target A	DA.2B	0.2	point mutation	NA	88	12	N/A	13.6
Chr13 target A	DA.2B	129	humanization with point mutation	23	176	24	N/A	13.6
C1Q[a]	*C1Q* KO	164	humanization	22/17	176	14	N/A	8

Each line represents a single electroporation. Top: targeted clones were produced by electroporation of targeting vectors alone. Middle: comparisons of targeting efficiency with or without co-electroporation of CRISPR reagents. Bottom: targeted clones were produced solely by co-electroporation of targeting vectors and CRISPR reagents. See also Tables S4, S5, and S6 and Figure S1.

[a]Row represents experiments re-targeted into previously modified clones.

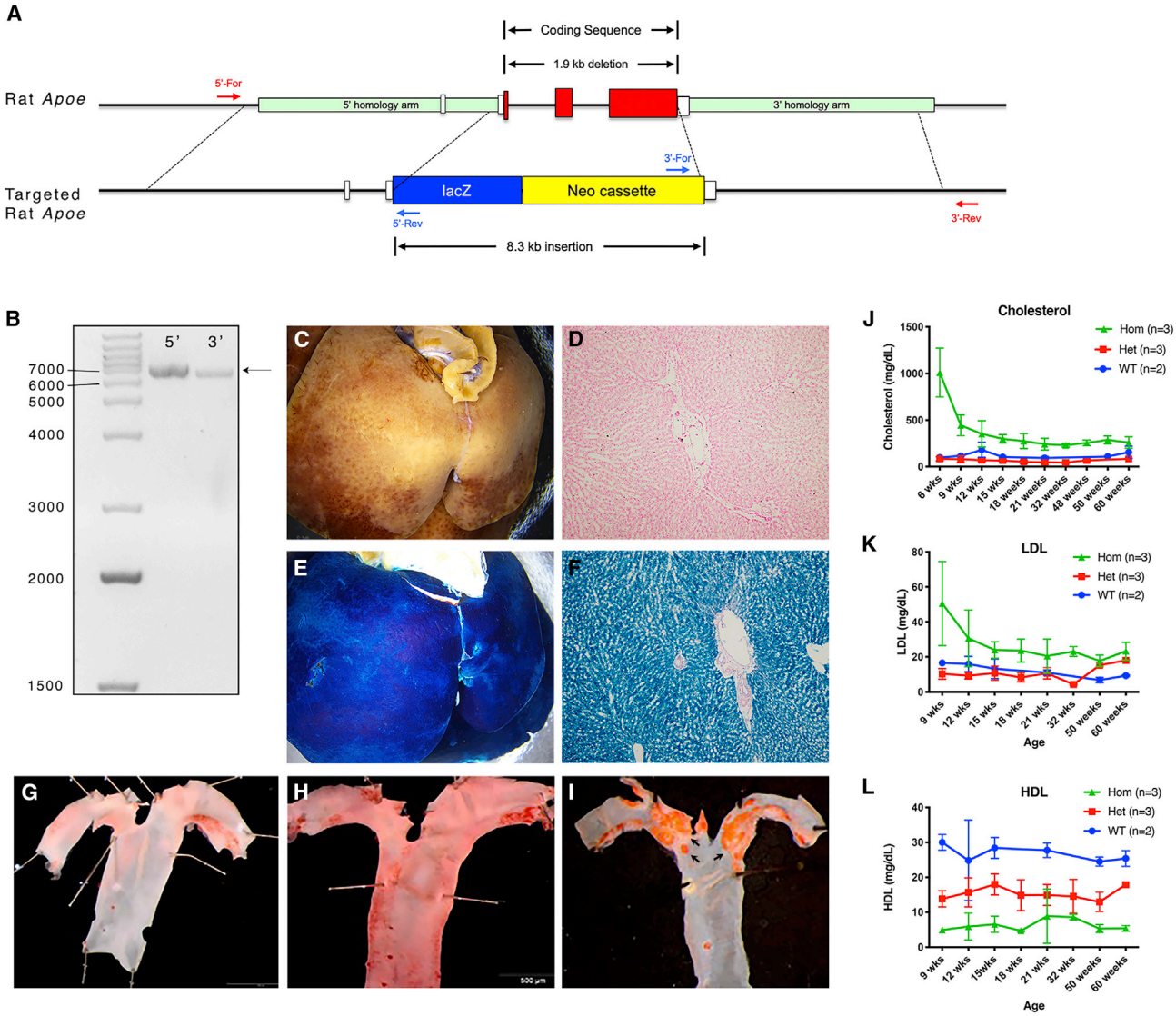

Figure 2. Phenotyping *Apoe* KO rats

(A) Design of the *Apoe* KO targeting vector. The entire coding sequence of the rat *Apoe* gene is replaced by a promoterless *lacZ* reporter and a neomycin selection cassette. PCR oligos are indicated.

(B) PCR gel confirming targeting of the *Apoe* locus (arrow; expected band sizes are in Table S7).

(C–F) X-gal staining for LacZ activity. 2 WT and 3 $Apoe^{+/-}$ animals were assayed. (C) WT sibling, liver. (D) WT sibling, section through liver. (E) $Apoe^{+/-}$ liver. (F) $Apoe^{+/-}$ section through liver.

(G–I) Oil red staining of aortas to detect atherosclerotic plaques. All animals were fed a high-fat diet. (G) WT rat, no plaques (n = 3). (H) $Apoe^{-/-}$ rat; little to no plaques (n = 3).

(I) $Apoe^{-/-}$ mouse: extensive plaques (arrows; n = 3).

(J–L) Serum chemistry for $Apoe^{-/-}$ rats. (J) Cholesterol. (K) Low-density lipoprotein (LDL). (L) High-density lipoprotein (HDL). Hom (n = 3): $Apoe^{-/-}$; Het (n = 3): $Apoe^{+/-}$; WT (n = 2): $Apoe^{+/+}$. Dots indicate mean values, brackets are +/− 1 standard deviation.

See also Tables S5 and S7; Figure S3.

To overcome this limitation, we used rESCs to produce *hNtrk2* rats. We designed an LTVEC that deletes the extracellular domain of the rat *Ntrk2* gene (~68 kb) and replaces it with the human extracellular domain (~74 kb; Figure 4A), thus producing a chimeric receptor that recognizes the human NTRK2 agonist antibody while maintaining the ability to activate the downstream rat signaling pathway. Targeting was confirmed by TaqMan and junction PCRs (Figures 4B and S3). We established a *hNtrk2* rat line by GLT of microinjected rESCs (Table S3) and used these rats

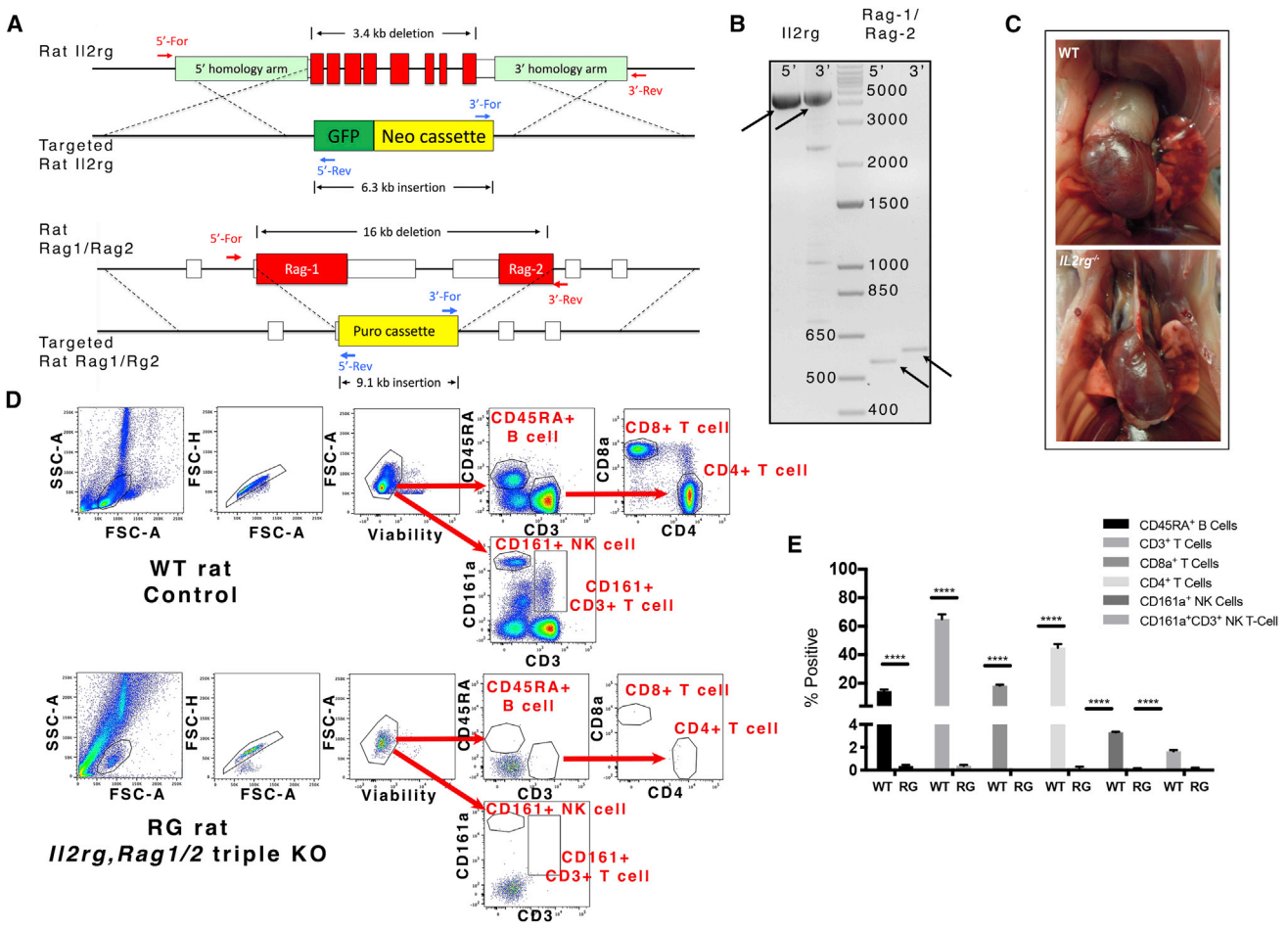

Figure 3. Phenotyping immunodeficient rats

(A) Design of the *Il2rg* KO and *Rag1/2* double KO (DKO) targeting vectors. PCR oligos are indicated.

(B) PCRs showing correct targeting of both alleles (arrows; expected band sizes are in Table S7).

(C) Gross dissection of WT control rats compared with *Il2rg* KO reveals hypoplastic thymus in *Il2rg* KO.

(D) FACS gating strategy for WT and RG rats.

(E) Summary of cell populations analyzed by FACS analysis in RG rats (n = 3 per group, males 12–20 weeks old). ****p < 0.0001.

See also Tables S5 and S7.

for antibody validation studies. Expression of the hNTRK2 protein in rats was comparable to that of the WT rat NTRK2 protein (Figures 4C and 4D).

To assess the effect of the NTRK2 agonist antibody on retinal ganglion cell (RGC) survival *in vivo*, we used a complete optic nerve transection model. Three and 10 days after transection, we injected 10 μg of our internally produced NTRK2 agonist antibody or isotype control intravitreally into one eye of *hNtrk2* rats. Animals were euthanized 14 days after axotomy (Figure 4E). We assessed the density of surviving RGCs after optic nerve transection in retinal whole mounts by immunofluorescence with an anti-BRN3A antibody (Figures 4F and 4G). We found that in Hom *hNtrk2* rats, the NTRK2 agonist antibody significantly ($p < 0.0001$, unpaired t test with Welch's correction) increased RGC survival compared with an isotype antibody control. (654 ± 30 versus 237 ± 26 RGCs per mm^2, mean ± SEM; Figures 4J and 4K). In *hNtrk2* mice, there is no effect on RGC survival (551 ± 30 versus 447 ± 26 RGCs per mm^2; Figures 3H and 3I), even when 40 μg NTRK2 agonist antibody was injected. In conclusion, the NTRK2 agonist antibody (H4H9780P) significantly increased RGC survival in *hNtrk2* rats but not *hNtrk2* mice.

DISCUSSION

Gene targeting in rats expands the landscape for modeling human diseases in rodents and provides a versatile

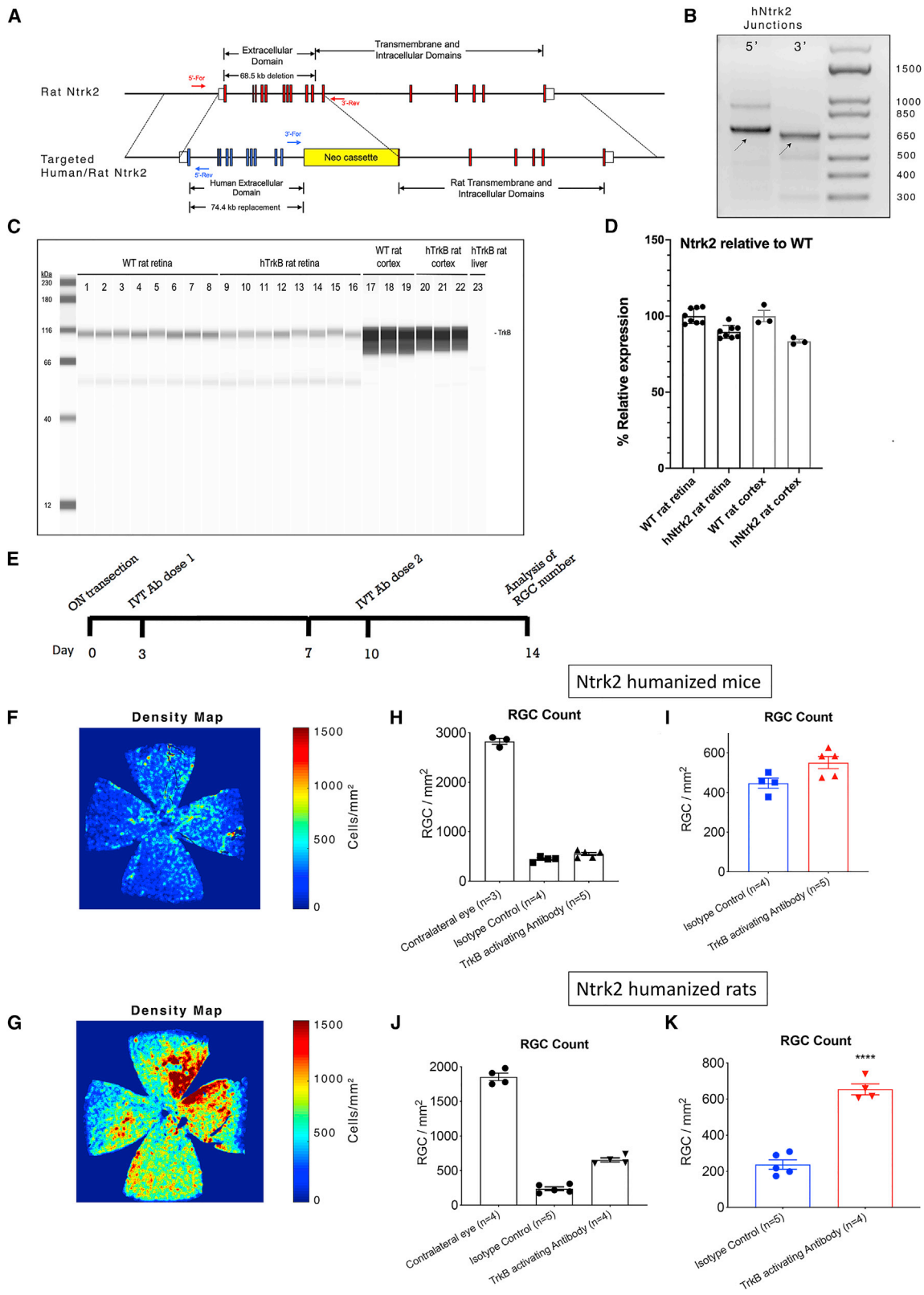

(legend on next page)

platform for the preclinical evaluation of fully human antibodies as biotherapeutics. Gene editing in 1-cell embryos using the CRISPR-Cas9 system has accelerated the production of rat models, but this method has disadvantages, mostly notably limitations on the size, precision, and category of modifications that are currently possible. While there have been reports of large deletions in rat embryos (Birling et al., 2017; Yoshimi et al., 2016), deletions are often imprecise, and humanizations are rare. We have demonstrated precise large-scale modifications of rESCs and the production of genetically modified rats following rESC microinjection, including the humanization of entire genes spanning up to 101 kb. BAC-based vectors remain the method of choice for large modifications to humanize mESCs; we have successfully adapted that technology for use in rESCs. We are also able to sequentially target separate genes, which enables efficient production of complex genotypes without time-consuming breeding steps while reducing the overall number of animals used to generate these genotypes.

Early reports on the derivation of rESCs enumerated several challenges to their utility. These challenges included genomic instability, tendencies to differentiate, weak or absent adherence to fibroblast feeder layers, and poor GLT (Buehr et al., 2008; Li et al., 2008; Ueda et al., 2008). Using a simple prescreening step, we could select high-quality candidate lines for karyotyping; 86% of these lines were euploid (Figure S1). We periodically karyotype our parental cell lines and have not seen changes in karyotype, self-renewal, or pluripotency even after 15–20 passages (data not shown). We have never seen significant differentiation when we culture our rESCs in 2i media, perhaps because we precultured the blastocysts with the 2i inhibitors prior to plating. Routine handling and passaging of our cells as floating colonies is not difficult. Indeed, the preparation of rESCs for microinjection is simpler and easier than mESCs because the collection of floating colonies eliminates contaminating fibroblasts in the microinjection prep. We have achieved GLT for all projects attempted thus far. Future work will seek to refine our culture methods with the goal of improving GLT.

Rats also offer technical advantages in terms of their physiology and size compared with mice. For example, we made *Apoe* KO rats to facilitate tissue collection and molecular analysis in an atherosclerosis model. Genetically modified rats may also open new areas of investigation. *Apoe* KO rats showed severely elevated serum cholesterol and LDL at a young age, but, to our surprise, serum cholesterol levels declined over time and stabilized at 2–3 times above WT levels. Even more surprising, after 12 weeks of high-fat diet, the *Apoe* KO rats rarely developed aortic plaques. This suggests that rats have some previously unsuspected mechanisms to control cholesterol/LDL levels and to counter atherosclerosis. These results warrant further investigation.

Genetically modified rat models may reproduce the characteristics of human diseases more accurately than mouse models do. NTRK2 is important for neuronal survival, differentiation and function, and NTRK2 agonists could have therapeutic potential in numerous neurological, mental, and metabolic disorders. A rodent model expressing the human target of human-NTRK2-targeting antibodies enables studies of the efficacy and mode of action of such agents in live animals as well as pharmacokinetic and pharmacodynamic studies. NTRK2 agonist antibodies had no effect in *hNtrk2* mice, whereas they were potently neuroprotective in the *hNtrk2* rats, possibly due to the larger size of rat eyes. It is also possible that the genetic background of the rats used in this study contributed to the rats' response to the NTRK2 agonist antibody. This model provides powerful validation for an exciting preclinical drug candidate in a small-animal model.

rESC derivation also opens up new possibilities for technology development. Because rESCs are pluripotent, it is possible to differentiate them into many mature cell types. Also, there are many inbred strains of rats that have been

Figure 4. *Ntrk2* agonist is neuroprotective in retinas of humanized *Ntrk2* rats but not humanized *Ntrk2* mice

(A) *Ntrk2* humanization vector. The extracellular domain of the rat *Ntrk2* gene is replaced by the homologous human domain and a selection cassette. Genotyping PCR oligonucleotides (oligos) are indicated.

(B) Junction PCRs showing correct targeting in rESCs (arrows; expected band sizes are in Table S7).

(C) Western blot with anti-NTRK2 pan-specific antibody. Each lane is a biological replicate. Lanes 1–16: WT or humanized NTRK2 (hNTRK2) rat retinas, as labeled. Lanes 17–22: WT or hNTRK2 rat cortex, as labeled. Lane 23: hNTRK2 rat liver.

(D) hNTRK2 quantified protein expression using ProteinSimple system.

(E) NTRK2 agonist antibody testing by intravitreal (IVT) injection following ON transection.

(F and G) BRNB3 staining of flat-mount retinal preps in humanized *Ntrk2* rats.

(F) Isotype control.

(G) NTRK2-agonist antibody.

(H and I) RGC counts in retinas of *hNtrk2* mice.

(J and K) RGC counts in retinas of *hNtrk2* rats.

RGC, retinal ganglion cells. Data points in (H)–(K) are biological replicates.

See also Table S5 and Figures S3 and S4.

developed to mimic certain human diseases, such as hypertension. rESC derivation is a straightforward process; it should be possible to derive a series of lines with unique genetic backgrounds in order to facilitate disease modeling in clinically relevant genetic backgrounds.

EXPERIMENTAL PROCEDURES

Resource availability

Corresponding author

Further information and requests for reagents should be directed to Jeffrey Lee (jeffrey.lee@regeneron.com).

Materials availability

Regeneron materials described in this resource may be available to qualified, academic, non-commercial researchers upon request, with minimal restrictions, subject to reasonable payments for maintenance and transport of materials, upon signing a Materials Transfer Agreement (MTA). Requests for materials may be made through our portal (https://regeneron.envisionpharma.com/ienv_research/visiontracker/portal/login.xhtml?pgm=ISR&windowId=4d6). Regeneron does not share clinical molecules. We do share alternative molecules that behave in a similar manner. For any questions about how we share our materials, please connect with us using the preclinical collaborations e-mail address (preclinical.collaborations@regeneron.com).

Data and code availability

No large datasets were generated in this study. No new code was generated in this study.

Tissue culture media

KSOM, M2 media, laminin, and chicken serum were purchased from Millipore Sigma (Burlington, MA, USA). mR1ECM was purchased from Cosmo Bio (Carlsbad, CA, USA). 2i media was prepared in house. DMEM-F12, neurobasal media, N2 and B27 supplements, and leukemia inhibitory factor (LIF) were purchased from Thermo Fisher Scientific (Waltham, MA, USA). PD0325901, CHIR99021, and Y-27632 were purchased from Reagents Direct (Encinitas, CA, USA). Fetal bovine serum (FBS) was purchased from Gemini (West Sacramento, CA, USA).

Animals

Animals were housed and all procedures were conducted in accordance with the ARVO Statement for Use of Animals in Ophthalmic and Vision Research and the Regeneron IACUC. SD rats were purchased from Taconic Biosciences. ACI rats were purchased from Charles River Laboratories.

rESC derivation

Frozen 8-cell- or blastocyst-stage embryos were purchased from Charles River Laboratories. Embryos were thawed and cultured in embryo culture dishes until cavitated. For fresh derivations, 5-week-old ACI females were superovulated using standard methods (Filipiak and Saunders, 2006). Embryos were flushed at the blastocyst stage. Cavitated embryos were treated with Acid Tyrodes to remove the zona pellucida; individual embryos were plated onto MEFs in a 96-well plate. Embryos were cultured in 2i media, and outgrowths were dissociated and replated into 24-well plates with MEFs with 2i media. Colonies were dissociated and replated into 6-well plates. Six-well colonies were dissociated and frozen for future use.

rESC daily handling

rESCs were cultured in 2i medium. rESCs were plated at a density of 1.0–1.5 × 10^5 cells/cm^2 onto a monolayer of mitotically inactivated MEFs. rESCs were incubated in a 37°C, 7.5% CO_2 incubator. rESC colonies grew as floating or loosely attached spheres. Media were changed daily. Spent media and rESC colonies were collected from the culture plate into 15 mL Falcon tubes and centrifuged for 5 min at 350 g; a minimal volume of spent media were left in the culture plate to prevent the MEFs from drying. After centrifugation, the supernatant was collected and discarded. Fresh media were added, and the rESC colonies were gently resuspended and replaced into the culture plate; a fresh feeder plate was used if the MEF monolayer was damaged or thin. rESCs were passaged every 4–5 days.

To passage rESCs, colonies were collected and pelleted as for daily feeding. The pellet was resuspended in 1 mL 0.05% Trypsin-EDTA and incubated for 1–15 min at 37°. One mL 2i media + 10% FBS was added to neutralize the trypsin. The cells were counted, diluted in 2i media, and plated at a density of 1.0–1.5 × 10^5 cells/cm^2 onto new feeder plates. To freeze cells, 0.5–1.0 × 10^6 cells were resuspended in 400 mL 90% FBS/10% DMSO, aliquoted into vials, and stored at −80°C.

rESC karyotyping

rESCs at passage 4 (P4)–P5 were treated for 1 h with 0.33 μg/mL colcemid to induce metaphase arrest. Colonies were dissociated, resuspended in 0.4% KCl, and incubated for 20 min at 37°. Cells were fixed in methanol/acetic acid (3:1), dropped onto glass slides, and dried for 60 min. Metaphase spreads were Giemsa stained and imaged; chromosomes were counted for 10–20 spreads per line. Lines in which >80% of spreads had close to 44 chromosomes were then expanded to P4–P7 and sent to the Coriell Institute for Medical Research (Camden, NJ, USA) for karyotyping. Lines were designated euploid if at least 80% of spreads showed a normal 42X,Y or 42X,X karyotype.

Antibodies

Primary antibodies included the following: OCT-4: BD Biosciences #611203; NANOG: Abcam #ab80892; SOX-2: Abcam #ab97959; REX1: Sigma #SAB2501302; TBX3: Sigma #SAB1409727; GATA6:R&D:MAB1700 at dilutions of 1:200. Secondary antibodies included the following: Invitrogen donkey anti-rabbit and anti-mouse 488 and anti-goat 594 (#A-21206, A021202, A11058) at 1:500.

Production of targeted rESC clones

rESCs were passaged 48 h before electroporation and cultured in 2i + 10 μM Y-27632. rESC colonies were trypsin dissociated for 10 min followed by serum inactivation. For LTVECs, 4 × 10^6 cells were electroporated with 2 μg vector using a BTX ECM 630 electroporation system (BTX, Holliston, MA, USA). For CRISPR projects,

2.5 μg of each sgRNA was mixed together and incubated with 20 μg Cas9 protein for 15 min at room temperature. RNPs were added to 2×10^6 rESCs and electroporated using the Lonza 4D-Nucleofector X Unit system (Lonza, Basel, Switzerland). For CRISPR-assisted homology-directed repair (HDR) projects, the RNP/cell mix was combined with 0.4 μg LTVEC prior to nucleofection. After transfection the cells were plated overnight in 2i media, followed by antibiotic resistance selection in one of the following conditions: G418 (75 μg/mL, 3 cycles of 2 days selection +1 day recovery), hygromycin (50 μg/mL for 5 days), or puromycin (0.75 μg/mL for 10 days).

Identification of targeted rESC clones

After selection, rESC colonies were picked and expanded in individual wells of a 96-well plate. Clones were dissociated and split into a freezing plate, stored at −150°C, and a laminin-coated screening plate. DNA was extracted from each screening plate well via automated lysis and binding with MagneSil RED (Promega, cat. A1641) on a Biomek FX liquid handling system. Screening for targeted ESC clones was done using TaqMan (Applied Biosystems) qPCR assays in a Thermo Fisher ViiA 7 Real-Time PCR System to determine the C_T for each reaction (the point in the PCR at which the fluorescence signal reached a preset threshold). C_T was used to determine loss of native allele by counting a reduction in intact copies of the target allele compared with copies of a reference gene (Valenzuela et al., 2003). Representative copy-number charts for two targets are shown in Figure S3. Sequences for genotyping assays are provided in Table S5. Positive clones were expanded for reconfirmation and blastocyst microinjection.

rESC microinjection

Eight-week-old SD female rats were subcutaneously injected with 40 μg LHRHa (Sigma) to synchronize estrus. Four days before implantation, synchronized female rats were mated overnight to vasectomized male SD rats; the following morning, females showing the presence of a vaginal plug were used for blastocyst transfer. Frozen SD blastocysts were purchased from Charles River Laboratories. On transfer day, frozen blastocysts were thawed in M2 media and incubated in KSOM at 37° for 2 h to allow recovery and expansion. rESC colonies were dissociated, and ∼15 cells were injected into the blastocoel of each blastocyst. Twelve to fourteen blastocysts were transplanted into each recipient. Male chimeras were test bred to SD female rats, and F1 founders were bred to establish each targeted line.

Intraorbital optic nerve axotomy and intravitreal injection

The left optic nerve (ON) was exposed intraorbitally, and its dura was opened. The ON was transected 1.5 mm behind the globe. Intravitreal injections were performed posterior to the pars plana with a pulled glass pipette connected to a 50 μL Hamilton syringe. Rats with postoperative complications (e.g., retinal ischemia, cataract) were excluded from further analysis. Animals in the control group received an isotype control antibody; the experimental group received the α-human NTRK2 antibody H4H9780 P at 3 and 10 days after ON axotomy. Rats were sacrificed 14 days after axotomy.

Counting viable RGCs

For BRN3A (a marker for surviving RGCs [Nadal-Nicolas et al., 2009]) immunostaining, retinas were blocked in 10% normal donkey serum and 0.5% Triton X-100 for 1 h and incubated in the same medium with BRN3A antibody (1:400; cat. sc-31984, Santa Cruz) overnight at 4°C, followed by anti-goat secondary for 2 h at room temperature.

NTRK2 western blots

Four WT and 4 *hNtrk2* rats were sacrificed at 8 months; retina and cortex were dissected and lysed with radioimmunoprecipitation assay (RIPA) buffer (Rockland #MB-030-0050) containing protease inhibitor cocktail (Sigma #P8340). Tissue lysates (12 μg each) were loaded into a ProteinSimple automated western blotting system, separated by size, and detected with anti-Ntrk2 antibody (Cell Signaling, #4603) by chemiluminescent reaction.

Statistical analysis

Statistical analysis was performed using statistical software (GraphPad Prism Software, San Diego, CA, USA). RGC numbers from different groups were analyzed by one-way analysis of variance (ANOVA). Dunnett's posthoc test was used to compare mean values of experimental groups against the same control group; Bonferroni's posttest was used to compare mean values for all groups.

SUPPLEMENTAL INFORMATION

Supplemental information can be found online at https://doi.org/10.1016/j.stemcr.2022.11.012.

AUTHOR CONTRIBUTIONS

Conceptualization, J.L., Y.H., C.R., and W.A.; methodology, J.L., J.W., R A., A.M., J.M., and Y.H.; investigation, J.L., J.W., R.A., S.T., J.H., L.M., B.M., J.S., A.A., A.L., and H.C.; writing – original draft, J.L. and Y.H.; writing – review & editing, J.L., E.C., B.Z., and W.A.; resources, J.L., R.A., A.M., C.B., and Y.H.; visualization, J.L., R.A., L.M., B.M., J.S., and H.C.; supervision, J.L., J.M., E.C., Y.H., D.V., C.R., B.Z., and W.A.

ACKNOWLEDGMENTS

We are grateful to Dr. Jean Siao and Dr. David Frendewey for helpful discussions.

CONFLICT OF INTERESTS

All authors are current or former employees and shareholders of Regeneron Pharmaceuticals. This work is related to patents US 10,894,965 (J.L., W.A., D.V.) and US 10,975,390 (J.L., W.A., A.M., D.V.).

Received: June 30, 2021
Revised: November 14, 2022
Accepted: November 15, 2022
Published: December 15, 2022

REFERENCES

Aiba, A., and Nakao, H. (2007). Conditional mutant mice using tetracycline-controlled gene expression system in the brain. Neurosci. Res. *58*, 113–117. https://doi.org/10.1016/j.neures.2007.01.009.

Amos-Landgraf, J.M., Kwong, L.N., Kendziorski, C.M., Reichelderfer, M., Torrealba, J., Weichert, J., Haag, J.D., Chen, K.S., Waller, J.L., Gould, M.N., and Dove, W.F. (2007). A target-selected Apc-mutant rat kindred enhances the modeling of familial human colon cancer. Proc. Natl. Acad. Sci. USA *104*, 4036–4041. https://doi.org/10.1073/pnas.0611690104.

Bai, Y., Xu, J., Brahimi, F., Zhuo, Y., Sarunic, M.V., and Saragovi, H.U. (2010). An agonistic TrkB mAb causes sustained TrkB activation, delays RGC death, and protects the retinal structure in optic nerve axotomy and in glaucoma. Invest. Ophthalmol. Vis. Sci. *51*, 4722–4731. https://doi.org/10.1167/iovs.09-5032.

Baker, H.J., Lindsey, J.R., and Weisbroth, S.H. (1979). The Laboratory Rat (Academic Press).

Birling, M.C., Schaeffer, L., André, P., Lindner, L., Maréchal, D., Ayadi, A., Sorg, T., Pavlovic, G., and Hérault, Y. (2017). Efficient and rapid generation of large genomic variants in rats and mice using CRISMERE. Sci. Rep. *7*, 43331. https://doi.org/10.1038/srep43331.

Brenin, D., Look, J., Bader, M., Hübner, N., Levan, G., and Iannaccone, P. (1997). Rat embryonic stem cells: a progress report. Transplant. Proc. *29*, 1761–1765. https://doi.org/10.1016/s0041-1345(97)00046-8.

Bronson, S.K., and Smithies, O. (1994). Altering mice by homologous recombination using embryonic stem cells. J. Biol. Chem. *269*, 27155–27158.

Buehr, M., Meek, S., Blair, K., Yang, J., Ure, J., Silva, J., McLay, R., Hall, J., Ying, Q.L., and Smith, A. (2008). Capture of authentic embryonic stem cells from rat blastocysts. Cell *135*, 1287–1298. https://doi.org/10.1016/j.cell.2008.12.007.

Capecchi, M.R. (1989). Altering the genome by homologous recombination. Science *244*, 1288–1292. https://doi.org/10.1126/science.2660260.

Chao, M.V. (2003). Neurotrophins and their receptors: a convergence point for many signalling pathways. Nat. Rev. Neurosci. *4*, 299–309. https://doi.org/10.1038/nrn1078.

Chazaud, C., Yamanaka, Y., Pawson, T., and Rossant, J. (2006). Early lineage segregation between epiblast and primitive endoderm in mouse blastocysts through the Grb2-MAPK pathway. Dev. Cell *10*, 615–624. https://doi.org/10.1016/j.devcel.2006.02.020.

Daniels, T.F., Killinger, K.M., Michal, J.J., Wright, R.W., Jr., and Jiang, Z. (2009). Lipoproteins, cholesterol homeostasis and cardiac health. Int. J. Biol. Sci. *5*, 474–488. https://doi.org/10.7150/ijbs.5.474.

Doetschman, T., Gregg, R.G., Maeda, N., Hooper, M.L., Melton, D.W., Thompson, S., and Smithies, O. (1987). Targetted correction of a mutant HPRT gene in mouse embryonic stem cells. Nature *330*, 576–578. https://doi.org/10.1038/330576a0.

Evans, M.J., and Kaufman, M.H. (1981). Establishment in culture of pluripotential cells from mouse embryos. Nature *292*, 154–156. https://doi.org/10.1038/292154a0.

Filipiak, W., and Saunders, T. (2006). Advances in transgenic rat production. Transgenic Res *15*, 673–686. https://doi.org/10.1007/s11248-006-9002-x.

Gusarova, V., Alexa, C.A., Wang, Y., Rafique, A., Kim, J.H., Buckler, D., Mintah, I.J., Shihanian, L.M., Cohen, J.C., Hobbs, H.H., et al. (2015). ANGPTL3 blockade with a human monoclonal antibody reduces plasma lipids in dyslipidemic mice and monkeys. J. Lipid Res. *56*, 1308–1317. https://doi.org/10.1194/jlr.M054890.

Jacob, H.J. (2010). The rat: a model used in biomedical research. Methods Mol. Biol. *597*, 1–11. https://doi.org/10.1007/978-1-60327-389-3_1.

Jaisser, F. (2000). Inducible gene expression and gene modification in transgenic mice. J. Am. Soc. Nephrol. *11* (*Suppl 16*), S95–S100.

Lau, J., Minett, M.S., Zhao, J., Dennehy, U., Wang, F., Wood, J.N., and Bogdanov, Y.D. (2011). Temporal control of gene deletion in sensory ganglia using a tamoxifen-inducible Advillin-Cre-ERT2 recombinase mouse. Mol. Pain *7*, 100. https://doi.org/10.1186/1744-8069-7-100.

Li, C., Yang, Y., Gu, J., Ma, Y., and Jin, Y. (2009). Derivation and transcriptional profiling analysis of pluripotent stem cell lines from rat blastocysts. Cell Res. *19*, 173–186. https://doi.org/10.1038/cr.2008.301.

Li, P., Tong, C., Mehrian-Shai, R., Jia, L., Wu, N., Yan, Y., Maxson, R.E., Schulze, E.N., Song, H., Hsieh, C.L., et al. (2008). Germline competent embryonic stem cells derived from rat blastocysts. Cell *135*, 1299–1310. https://doi.org/10.1016/j.cell.2008.12.006.

Macdonald, L.E., Karow, M., Stevens, S., Auerbach, W., Poueymirou, W.T., Yasenchak, J., Frendewey, D., Valenzuela, D.M., Giallourakis, C.C., Alt, F.W., et al. (2014). Precise and in situ genetic humanization of 6 Mb of mouse immunoglobulin genes. Proc. Natl. Acad. Sci. USA *111*, 5147–5152. https://doi.org/10.1073/pnas.1323896111.

Martin, G.R. (1981). Isolation of a pluripotent cell line from early mouse embryos cultured in medium conditioned by teratocarcinoma stem cells. Proc. Natl. Acad. Sci. USA *78*, 7634–7638. https://doi.org/10.1073/pnas.78.12.7634.

Mashimo, T., Takizawa, A., Kobayashi, J., Kunihiro, Y., Yoshimi, K., Ishida, S., Tanabe, K., Yanagi, A., Tachibana, A., Hirose, J., et al. (2012). Generation and characterization of severe combined immunodeficiency rats. Cell Rep. *2*, 685–694. https://doi.org/10.1016/j.celrep.2012.08.009.

Massimi, M., Lear, S.R., Williams, D.L., Jones, A.L., and Erickson, S.K. (1999). Differential expression of apolipoprotein E messenger RNA within the rat liver lobule determined by in situ hybridization. Hepatology *29*, 1549–1555. https://doi.org/10.1002/hep.510290504.

Meek, S., Buehr, M., Sutherland, L., Thomson, A., Mullins, J.J., Smith, A.J., and Burdon, T. (2010). Efficient gene targeting by homologous recombination in rat embryonic stem

cells. PLoS One *5*, e14225. https://doi.org/10.1371/journal.pone.0014225.

Meir, K.S., and Leitersdorf, E. (2004). Atherosclerosis in the apolipoprotein-E-deficient mouse: a decade of progress. Arterioscler. Thromb. Vasc. Biol. *24*, 1006–1014. https://doi.org/10.1161/01.ATV.0000128849.12617.f4.

Men, H., Bauer, B.A., and Bryda, E.C. (2012). Germline transmission of a novel rat embryonic stem cell line derived from transgenic rats. Stem Cell. Dev. *21*, 2606–2612. https://doi.org/10.1089/scd.2012.0040.

Ménoret, S., Iscache, A.L., Tesson, L., Rémy, S., Usal, C., Osborn, M.J., Cost, G.J., Brüggemann, M., Buelow, R., and Anegon, I. (2010). Characterization of immunoglobulin heavy chain knockout rats. Eur. J. Immunol. *40*, 2932–2941. https://doi.org/10.1002/eji.201040939.

Morrison, J.C., Johnson, E., and Cepurna, W.O. (2008). Rat models for glaucoma research. In Glaucoma: An Open Window to Neurodegeneration and Neuroprotection, pp. 285–301. https://doi.org/10.1016/s0079-6123(08)01121-7.

Murphy, A.J., Macdonald, L.E., Stevens, S., Karow, M., Dore, A.T., Pobursky, K., Huang, T.T., Poueymirou, W.T., Esau, L., Meola, M., et al. (2014). Mice with megabase humanization of their immunoglobulin genes generate antibodies as efficiently as normal mice. Proc. Natl. Acad. Sci. USA *111*, 5153–5158. https://doi.org/10.1073/pnas.1324022111.

Nadal-Nicolás, F.M., Jiménez-López, M., Sobrado-Calvo, P., Nieto-López, L., Cánovas-Martínez, I., Salinas-Navarro, M., Vidal-Sanz, M., and Agudo, M. (2009). Brn3a as a marker of retinal ganglion cells: qualitative and quantitative time course studies in naive and optic nerve-injured retinas. Invest. Ophthalmol. Vis. Sci. *50*, 3860–3868. https://doi.org/10.1167/iovs.08-3267.

Nakashima, Y., Plump, A.S., Raines, E.W., Breslow, J.L., and Ross, R. (1994). ApoE-deficient mice develop lesions of all phases of atherosclerosis throughout the arterial tree. Arterioscler. Thromb. *14*, 133–140.

Plump, A.S., Smith, J.D., Hayek, T., Aalto-Setälä, K., Walsh, A., Verstuyft, J.G., Rubin, E.M., and Breslow, J.L. (1992). Severe hypercholesterolemia and atherosclerosis in apolipoprotein E-deficient mice created by homologous recombination in ES cells. Cell *71*, 343–353. https://doi.org/10.1016/0092-8674(92)90362-g.

Robertson, E., Bradley, A., Kuehn, M., and Evans, M. (1986). Germline transmission of genes introduced into cultured pluripotential cells by retroviral vector. Nature *323*, 445–448. https://doi.org/10.1038/323445a0.

Rongvaux, A., Takizawa, H., Strowig, T., Willinger, T., Eynon, E.E., Flavell, R.A., and Manz, M.G. (2013). Human hemato-lymphoid system mice: current use and future potential for medicine. Annu. Rev. Immunol. *31*, 635–674. https://doi.org/10.1146/annurev-immunol-032712-095921.

Smith, A.G. (2001). Embryo-derived stem cells: of mice and men. Annu. Rev. Cell Dev. Biol. *17*, 435–462. https://doi.org/10.1146/annurev.cellbio.17.1.435.

Stein, E.A., Mellis, S., Yancopoulos, G.D., Stahl, N., Logan, D., Smith, W.B., Lisbon, E., Gutierrez, M., Webb, C., Wu, R., et al. (2012). Effect of a monoclonal antibody to PCSK9 on LDL cholesterol. N. Engl. J. Med. *366*, 1108–1118. https://doi.org/10.1056/NEJMoa1105803.

Strowig, T., Rongvaux, A., Rathinam, C., Takizawa, H., Borsotti, C., Philbrick, W., Eynon, E.E., Manz, M.G., and Flavell, R.A. (2011). Transgenic expression of human signal regulatory protein alpha in Rag2-/-gamma(c)-/- mice improves engraftment of human hematopoietic cells in humanized mice. Proc. Natl. Acad. Sci. USA *108*, 13218–13223. https://doi.org/10.1073/pnas.1109769108.

Thomas, K.R., and Capecchi, M.R. (1987). Site-directed mutagenesis by gene targeting in mouse embryo-derived stem cells. Cell *51*, 503–512. https://doi.org/10.1016/0092-8674(87)90646-5.

Tong, C., Li, P., Wu, N.L., Yan, Y., and Ying, Q.L. (2010). Production of p53 gene knockout rats by homologous recombination in embryonic stem cells. Nature *467*, 211–213. https://doi.org/10.1038/nature09368.

Ueda, S., Kawamata, M., Teratani, T., Shimizu, T., Tamai, Y., Ogawa, H., Hayashi, K., Tsuda, H., and Ochiya, T. (2008). Establishment of rat embryonic stem cells and making of chimera rats. PLoS One *3*, e2800. https://doi.org/10.1371/journal.pone.0002800.

Vaira, S., Yang, C., McCoy, A., Keys, K., Xue, S., Weinstein, E.J., Novack, D.V., and Cui, X. (2012). Creation and preliminary characterization of a leptin knockout rat. Endocrinology *153*, 5622–5628. https://doi.org/10.1210/en.2012-1462.

Valenzuela, D.M., Murphy, A.J., Frendewey, D., Gale, N.W., Economides, A.N., Auerbach, W., Poueymirou, W.T., Adams, N.C., Rojas, J., Yasenchak, J., et al. (2003). High-throughput engineering of the mouse genome coupled with high-resolution expression analysis. Nat. Biotechnol. *21*, 652–659. https://doi.org/10.1038/nbt822.

Waite, J.C., Wang, B., Haber, L., Hermann, A., Ullman, E., Ye, X., Dudgeon, D., Slim, R., Ajithdoss, D.K., Godin, S.J., et al. (2020). Tumor-targeted CD28 bispecific antibodies enhance the antitumor efficacy of PD-1 immunotherapy. Sci. Transl. Med. *12*, eaba2325. https://doi.org/10.1126/scitranslmed.aba2325.

Walsh, N.C., Kenney, L.L., Jangalwe, S., Aryee, K.E., Greiner, D.L., Brehm, M.A., and Shultz, L.D. (2017). Humanized mouse models of clinical disease. Annu. Rev. Pathol. *12*, 187–215. https://doi.org/10.1146/annurev-pathol-052016-100332.

White, M.A., Nicolette, C., Minden, A., Polverino, A., Van Aelst, L., Karin, M., and Wigler, M.H. (1995). Multiple Ras functions can contribute to mammalian cell transformation. Cell *80*, 533–541. https://doi.org/10.1016/0092-8674(95)90507-3.

Ying, Q.L., Wray, J., Nichols, J., Batlle-Morera, L., Doble, B., Woodgett, J., Cohen, P., and Smith, A. (2008). The ground state of embryonic stem cell self-renewal. Nature *453*, 519–523. https://doi.org/10.1038/nature06968.

Yoshimi, K., Kunihiro, Y., Kaneko, T., Nagahora, H., Voigt, B., and Mashimo, T. (2016). ssODN-mediated knock-in with CRISPR-Cas for large genomic regions in zygotes. Nat. Commun. *7*, 10431. https://doi.org/10.1038/ncomms10431.

Yue, P., Averna, M., Lin, X., and Schonfeld, G. (2006). The c.43_44insCTG variation in PCSK9 is associated with low plasma

LDL-cholesterol in a Caucasian population. Hum. Mutat. *27*, 460–466. https://doi.org/10.1002/humu.20316.

Zhao, Y., Liu, P., Xin, Z., Shi, C., Bai, Y., Sun, X., Zhao, Y., Wang, X., Liu, L., Zhao, X., et al. (2019). Biological characteristics of severe combined immunodeficient mice produced by CRISPR/Cas9-Mediated Rag2 and IL2rg mutation. Front. Genet. *10*, 401. https://doi.org/10.3389/fgene.2019.00401.

Zijlstra, M., Li, E., Sajjadi, F., Subramani, S., and Jaenisch, R. (1989). Germ-line transmission of a disrupted beta 2-microglobulin gene produced by homologous recombination in embryonic stem cells. Nature *342*, 435–438. https://doi.org/10.1038/342435a0.